JOURNAL OF GEOPHYSICAL RESEARCH, VOL. 117, D10202, doi:10.1029/2011JD017161, 2012

Year-round radiocarbon-based source apportionment of carbonaceous aerosols at two background sites in South Asia

Rebecca J. Sheesley,[1,2] Elena Kirillova,[1] August Andersson,[1] Martin Kruså,[1] P. S. Praveen,[3,4] Krishnakant Budhavant,[5,6] P. D. Safai,[6] P. S. P. Rao,[6] and Örjan Gustafsson[1]

Received 14 November 2011; revised 12 March 2012; accepted 5 April 2012; published 23 May 2012.

[1] Atmospheric Brown Clouds (ABC), regional-scale haze events, are a significant concern for both human cardiopulmonary health and regional climate impacts. In order to effectively mitigate this pollution-based phenomenon, it is imperative to understand the magnitude, scope and source of ABC in regions such as South Asia. Two sites in S. Asia were chosen for a 15-month field campaign focused on isotope-based source apportionment of carbonaceous aerosols in 2008–2009. Both the Maldives Climate Observatory in Hanimaadhoo (MCOH) and a mountaintop site in Sinhagad, India (SINH) act as regionally mixed receptor sites. Annual radiocarbon-based source apportionment for soot elemental carbon (SEC) at MCOH and SINH revealed 73 ± 6% and 59 ± 5% contribution from biomass combustion, respectively (remainder from fossil fuel). The contributions from biogenic/biomass combustion to total organic carbon were similar between MCOH and SINH (69 ± 5% and 64 ± 5, respectively). The biomass combustion contribution for SEC in the current study, especially the results from MCOH, shows good agreement with published black carbon emissions inventories for India. Geographic source assessment, including clustered back trajectory analysis and carbon contribution by source region, indicated that the highest SEC/TOC loads originated from the W. Indian coastal margin, including the coastal city of Mumbai, India. The winter dry season ^{14}C-based source apportionment of the BC-tracing SEC fraction for 2006, 2008, 2009 were not statistically different ($p = 0.7$) and point to a near-constant two-thirds contribution from biomass combustion practices, including wood and other biofuels as well as burning of agricultural crop residues.

Citation: Sheesley, R. J., E. Kirillova, A. Andersson, M. Kruså, P. S. Praveen, K. Budhavant, P. D. Safai, P. S. P. Rao, and Ö. Gustafsson (2012), Year-round radiocarbon-based source apportionment of carbonaceous aerosols at two background sites in South Asia, *J. Geophys. Res.*, *117*, D10202, doi:10.1029/2011JD017161.

1. Introduction

[2] The high concentration of atmospheric particles during the dry season in South Asia has large implications both for human health and the regional climate [*Ramanathan et al.*, 2001; *U. N. Environmental Programme* (*UNEP*), 2008]. An important component of the particulate matter in S. Asia is black carbon (BC), formed from incomplete combustion from such diverse sources as wood burning, cooking, motor vehicle exhaust, coal combustion and residual crop burning. BC is a strong absorber of sunlight: heating the atmosphere, dimming the surface and potentially altering regional hydrological cycles [*Menon et al.*, 2002; *Ramanathan and Carmichael*, 2008]. The phenomenon of highly polluted air masses, particularly with high BC levels, has been termed Atmospheric Brown Clouds (ABC) due to their regional distribution and impact [*Ramanathan and Crutzen*, 2003]. While investigating the ABC phenomenon, there have been attempts to determine the relative impact of various combustion sources on total BC concentrations and climate forcing. It has been demonstrated that pollution from different combustion sources, as implied from BC-to-sulfate ratios and BC-to-organic-carbon (OC) ratios, can have unique solar absorption efficiencies [*Kirchstetter et al.*, 2004; *Sandradewi et al.*, 2008; *Ramana et al.*, 2010]. Thus

[1]Department of Applied Environmental Science and the Bert Bolin Centre for Climate Research, Stockholm University, Stockholm, Sweden.
[2]Now at Department of Environmental Science, Baylor University, Waco, Texas, USA.
[3]Maldives Climate Observatory at Hanimaadhoo, Hanimaadhoo, Maldives.
[4]Now at Center for Clouds, Chemistry and Climate, Scripps Institution of Oceanography, University of California, San Diego, La Jolla, California, USA.
[5]Vishwakarma Institute of Technology, Pune, India.
[6]Physical Meteorology and Aerology Division, Indian Institute of Tropical Meteorology, Pune, India.

Corresponding author: R. J. Sheesley, Department of Environmental Science, Baylor University, 1 Bear Pl., #97266, Waco, TX 76798-7266, USA. (rebecca_sheesley@baylor.edu)

0148-0227/12/2011JD017161

an investigation of source contribution is highly relevant in determining both the impact of and mitigation strategy for BC as a short-lived climate forcer.

[3] The region of South Asia has a population and an economy that is rapidly growing and changing [*Pucher et al.*, 2007]; this causes transitions in both technology and social demographics, which ultimately will have significant impacts on BC and OC emissions [*Bond et al.*, 2004; *Cole and Neumayer*, 2004; *Venkataraman et al.*, 2005; *O'Neill et al.*, 2010]. For example, there is rapid motorization demonstrated in India, particularly in urban areas [*Pucher et al.*, 2007]. Many previous studies have reported on BC and TOC concentrations in the ABC over S. Asia [*Novakov et al.*, 2000; *Lelieveld et al.*, 2001; *Dickerson et al.*, 2002; *Mayol-Bracero et al.*, 2002; *Neususess et al.*, 2002; *Corrigan et al.*, 2006; *Rengarajan et al.*, 2007; *Stone et al.*, 2007; *Gustafsson et al.*, 2009; *Ram and Sarin*, 2009; *Granat et al.*, 2010]. Previous source apportionment and emissions inventory studies in the region have reported a wide range of biomass/biofuel burning contributions to BC [*Lelieveld et al.*, 2001; *Dickerson et al.*, 2002; *Bond et al.*, 2004; *Stone et al.*, 2007; *Lawrence and Lelieveld*, 2010]. Because of the high potential for changes in emission sources and ambient concentrations, there is great value in continued long-term monitoring of both ambient levels and sources of carbonaceous aerosols in this rapidly changing region.

[4] The climate implications of BC emissions in S. Asia are considered of global importance, but the dynamics of the particulate carbon system are not well understood. There continue to be questions about the magnitude of BC emissions from S. Asia and the source provenance of those emissions [*Lawrence and Lelieveld*, 2010]. Previous efforts have estimated a wide range of possible contributions from biomass/biofuel burning and fossil fuel combustion which vary by campaign, by analytical methodology and by source apportionment technique [*Novakov et al.*, 2000; *Lelieveld et al.*, 2001; *Dickerson et al.*, 2002; *Mayol-Bracero et al.*, 2002; *Salam et al.*, 2003; *Stone et al.*, 2007]. Natural abundance radiocarbon (^{14}C) measurements offer an opportunity to quantitatively resolve between fossil fuel and modern biomass combustion sources of atmospheric BC [*Szidat et al.*, 2006; *Gustafsson et al.*, 2009; *Lawrence and Lelieveld*, 2010]. In a first short-term application of the ^{14}C technique to S. Asian aerosols, two fractions of BC were isolated from dry season samples at observatories located in the northern Indian Ocean and in W. India [*Gustafsson et al.*, 2009]. The advantage of the ^{14}C approach is that it has well-constrained end-member values spanning a large dynamic range (fossil carbon has no ^{14}C while contemporary carbon has a well-defined $^{14}C/^{12}C$). Furthermore, the $^{14}C/^{12}C$ ratio is an intrinsic property of the carbonaceous aerosol, which in contrast to molecular or elemental source tracers, is independent of concentration. For TOC, the fraction biomass naturally includes particulate matter from primary biogenic emissions, biomass combustion and secondary organic carbon from both biogenic and biomass combustion precursors. The fraction fossil (i.e., 1 – fraction biomass) for TOC reflects both fossil fuel combustion and secondary organic carbon from fossil precursors. In contrast, for BC, the fraction biomass can only arise from biomass combustion and the fossil contribution is likewise solely due to fossil fuel combustion.

[5] The same radiocarbon source apportionment protocol used in the short-duration pilot study [*Gustafsson et al.*, 2009] is employed in the current study but with a significantly expanded timeline and enhanced geographic source assessment. There is a clear need to constrain statistically the year-round-averaged sources of S. Asian aerosols in this transitioning region, as well as the inter-annual variability for the dry period (the key season for high loadings and environmental impacts). The current study comprehensively covers a 15 month period at two regional receptor sites in South Asia: Maldives Climate Observatory-Hanimaadhoo (MCOH) and Sinhagad, India (SINH). These sites were chosen as regional receptors with limited local influence and significant historical data set of BC concentrations. The majority of two dry seasons (2008 and 2009) and a single monsoon season are included in this 15 month period. Concentration and $^{13}C/^{14}C$-based source apportionment of total organic carbon (TOC) and soot elemental carbon (SEC) [*Zencak et al.*, 2007; *Gustafsson et al.*, 2009; *Andersson et al.*, 2011], a recalcitrant component of the BC continuum [*Elmquist et al.*, 2006], are presented. In addition to chemical-isotopic characterization, geographic source referencing combining back trajectory analysis with mean concentration has been accomplished to determine whether differences exist in emission source contributions from spatially resolved source regions in S. Asia.

2. Methods

2.1. Description of Sampling Sites

[6] Fifteen months-long ambient sampling campaigns were conducted at two regional receptor sites of the Atmospheric Brown Cloud (ABC) Programme (http://www.rrcap.unep.org/abc/) in South Asia: The Maldives Climate Observatory – Hanimaadhoo (MCOH: lat 6.78°N long 73.18°E) and Sinhagad, India (SINH: lat 18.35°N long 73.75°E). MCOH is located on the isolated northern tip of the small island of Hanimaadhoo (6.5 × 0.73 km), one of the northernmost islands of the Republic of the Maldives. MCOH is operated jointly by the Government of the Maldives (Environmental Protection Agency) and the UNEP-ABC Programme. This northern Indian Ocean site is ideally situated away from any significant local sources. In the winter dry period it is downwind of the Indian subcontinent, including Pakistan, India and Bangladesh. SINH is located at Sinhagad Fort, 1400 m above sea level and is operated by the Indian Institute of Tropical Meteorology (Pune, India). SINH is a high altitude site, representing primarily regionally mixed sources from west to central India with additional influence from the Indo-Gangetic Plains to the northeast. Both MCOH [*Corrigan et al.*, 2006; *Ramana and Ramanathan*, 2006; *Adhikary et al.*, 2007; *Holecek et al.*, 2007; *Stone et al.*, 2007; *Gustafsson et al.*, 2009; *Granat et al.*, 2010; *Ramana et al.*, 2010; *Sheesley et al.*, 2011] and SINH [*Momin et al.*, 2005; *Gustafsson et al.*, 2009; *Budhavant et al.*, 2011; *Coz and Leck*, 2011; *Raju et al.*, 2011], are frequently used for studies of S. Asian aerosols.

2.2. Sampling Program

[7] With the objective of apportioning aerosol sources, high-volume sampling of the total suspended particulate

matter (TSP) was conducted at each site from January 2008 to April 2009 using identical custom-built systems. TSP does not have a distinct size cut, but roughly collects particles 100 microns and less. These consisted of both a high-volume line, intended primarily to obtain sufficient amounts for ^{14}C analysis of various aerosol carbon fractions, and a low-volume line used for detailed concentration measurements. The high-volume sampling train operated at 14–19 m^3 h^{-1} and collected TSP on 140 mm quartz fiber filters (Tissuquartz filters from Pall Gelman). The low-volume sampling train operated at 9–12 l/min and collected TSP on 47 mm quartz fiber filters (Tissuquartz filters from Pall Gelman).

[8] Sampling duration at MCOH was approximately one week during the non-monsoon periods and two weeks during monsoon season. The more polluted SINH site was maintained at a near-constant 1 week sampling duration. This provided complete and synoptic coverage for nearly 15 months at both sites. Two sampling systems were operated at each site to ensure back-up for the continuous observations. Prior to the campaign, quartz fiber filters were pre-baked at 450°C for 12 h and individually stored in aluminum foil packets in double Ziploc bags in the freezer. Filter blanks were collected roughly once per month for each site (i.e., after every 2–4 samples), alternating sampling systems. All filters were kept in cold storage, preceding and following sampling in order to minimize contamination from organic compounds sorbing to the filter. For shipping, samples were encased in a third, sealed plastic bag to minimize contamination. All blanks were shipped, stored and processed in an identical manner as the samples.

2.3. Carbon Concentration

[9] Briefly, for TOC quantification, 2–6 punches (diameter = 0.48 cm) of each filter were placed in pre-baked silver capsules and then acidified with 1M hydrochloric acid. The capsules were then dried and analyzed for total organic carbon using an elemental analyzer interfaced with an isotope ratio mass spectrometer. This elemental analysis was performed by the Stable Isotope Facility at the University of California-Davis and the Stable Isotope Laboratory (Dept. of Geosciences) at Stockholm University. All reported TOC results were blank subtracted using an average filter blank for each site. For MCOH, the TOC blank (2.3 ± 1.8 sd, μg cm^2; n = 7) was 3% of the average filter loading. Triplicate analysis was done on every sixth filter. The relative standard deviation of the average of the triplicate analyses for TOC at MCOH was 3% (one outlier excluded). For SINH, the filter blank (2.9 ± 1.6 sd, μg cm^2; n = 11) was also 3% of the average loading and the relative standard deviation of triplicate analysis was 5%. The minimum detection limit was calculated across both sites as the average filter blank plus one standard deviation.

[10] The SEC content was determined using chemothermal oxidation at 375°C [*Gustafsson et al.*, 1997; *Elmquist et al.*, 2006; *Zencak et al.*, 2007]. Sixteen punches (diameter = 0.48 cm) of each 140 mm filter were placed in silver capsules and then heated at 375°C for 18 h under active airflow. The samples were then processed the same as the TOC: acidified, dried and analyzed by elemental analysis-isotope ratio mass spectrometry. All reported SEC results were blank subtracted using a campaign-average filter blank (central value 0.7 ± 0.6 sd, μg cm^2; n = 19). For SEC, blank levels were dominated by in-lab method contamination as opposed to field contamination as in the TOC blanks. The blank was 16% of the average filter loading, however there was a large range of measured filter loadings with high SEC during the dry season (average 5.4 μg cm^2) and very low SEC during the wet season (average 1.8 μg cm^2). Triplicate analysis was done roughly every sixth filter. The relative standard deviation of the triplicate analysis was 15%.

[11] Relative standard deviation for elemental analysis was <1%. Uncertainty for carbon analysis was calculated as average blank plus relative standard deviation of all triplicate analysis. This was calculated based on sample loading, not final concentration.

2.4. Carbon Isotopes Analysis

[12] For the accelerator mass spectrometry measurement of the ambient radiocarbon signal of TOC and SEC, the 140 mm filters were cut and composited to give 100–300 μg of carbon for SEC and 150–500 μg of carbon for TOC. Individual samples were analyzed for January–March 2008 and November–December 2009, two weeks were composited for April, four-six weeks were composited for May–October and two-four weeks were composited for January–April 2009 for TOC. The SEC compositing was roughly three weeks during non-monsoon winter and six-ten weeks during transitional and monsoon seasons. A detailed list for the compositing and the isotopic results are included in the auxiliary material (Tables S4 and S5 in Text S1).[1] Sub-sampling was designed such that equal mass of carbon were combined within each composite group to ensure that each filter sample was equally represented in the isotopic composition. For the TOC, these filter sections were then acidified in a desiccators over HCl and dried in a drying oven. For SEC, filter sections were placed in an aluminum boat and subjected to the chemothermal oxidation treatment followed by acidification in a desiccator as for TOC. The dried aerosol filters for ^{14}C analysis of TOC and SEC components were shipped to the U.S.-NSF National Ocean Sciences Accelerator Mass Spectrometry Facility (NOSAMS) in pre-baked, sealed glass petri dishes, as in previous studies [*Gustafsson et al.*, 2009]. Radiocarbon is reported from NOSAMS as F_{modern} (F_m). All radiocarbon results have been blank corrected using a site-specific filter blanks from MCOH and SINH with average 0.5 μg cm^2 loading per blank. The SEC blank for this campaign used a combination of filter blanks from MCOH and SINH which gave a F_m of 0.384 ± 0.007, similar to the SEC blank result from the 2006 (F_m = 0.33 for MCOH and F_m = 0.33 SINH). For TOC, the MCOH blank used for correction was F_m = 0.696 ± 0.009, while the SINH blank was F_m = 0.571 ± 0.012. The F_m of the SINH blank was confirmed by a second filter blank (F_m = 0.607 ± 0.003) and parallels the F_m of previously published ^{14}C TOC blanks (0.79 [*Bench and Herckes*, 2004]; 0.57 [*Gustafsson et al.*, 2009]).

[1] Auxiliary materials are available in the HTML. doi:10.1029/2011JD017161.

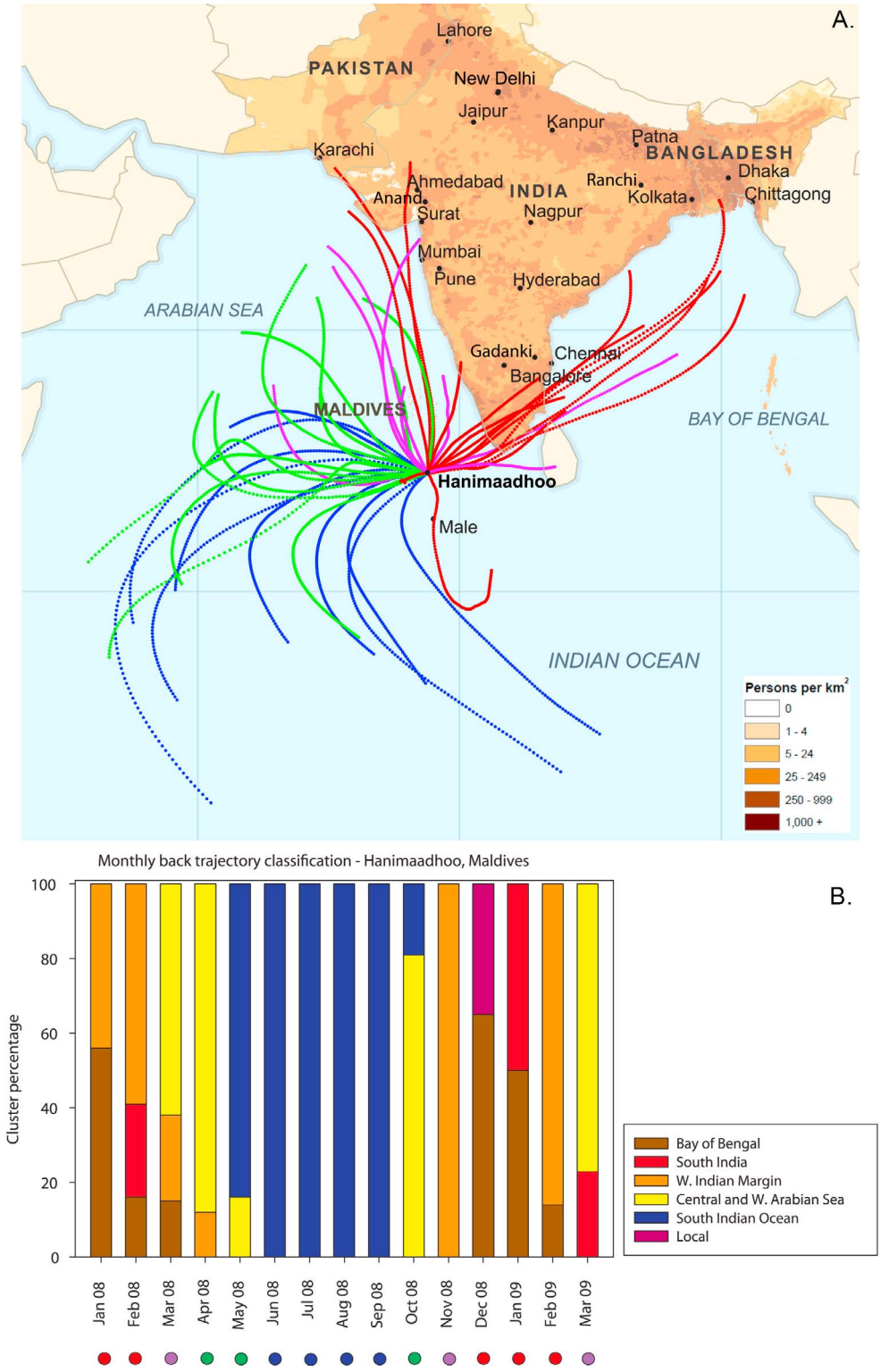

Figure 1. (a) Clustered 6-hourly, 5-day back trajectory means for Hanimaadhoo, Maldives (MCOH) Jan 08–Mar 09 (total n = 1744). The cluster means are colored to depict seasonal differences: winter is red (Jan, Feb, Dec); winter transition months are purple (Mar, Nov); pre- and post-monsoon are green (Apr, May, Oct); and monsoon is blue (Jun–Sept). (b) Source region classification for clustered back trajectories by month with seasons marked at bottom by colored dots.

[13] The carbon isotope results are presented in the paper using established protocols for presentation of carbon isotope results [*Stuiver and Polach*, 1977]. Briefly, stable carbon isotope results are presented as $\delta^{13}C$, the isotope ratio ($^{13}C/^{12}C$) of the sample relative to that of Vienna PeeDee Belemnite, while radiocarbon results are presented as an isotope ratio ($^{14}C/^{12}C$), normalized to a $\delta^{13}C$ of −25‰, relative to the NBS Oxalic Acid I standard as fraction modern (F_m), and decay corrected [*Stuiver and Polach*, 1977; *Zencak et al.*, 2007].

2.5. Radiocarbon-Based Source Apportionment

[14] The F_m reported by NOSAMS is first converted to $\Delta^{14}C$ using the following equation:

$$\Delta^{14}C_{sample} = 1000 * \left(F_{modern} * e^{(1/8267)*(1950-2008)} - 1\right). \quad (1)$$

[15] To calculate the contribution of modern biomass to TOC and SC during this study, a mass balance equation is used with $\Delta^{14}C = -1000‰$ as the end-member for fossil carbon and $\Delta^{14}C = +199‰$ for modern biomass [*Mandalakis et al.*, 2005; *Zencak et al.*, 2007; *Gustafsson et al.*, 2009]. The modern biomass end-member ($\Delta^{14}C_{biomass} = +199$) replicates an earlier study [*Gustafsson et al.*, 2009]. Briefly, it is based on relative contribution of wood fuel (83% at $\Delta^{14}C$ = +225‰) and dung plus crop waste (17% at $\Delta^{14}C = +70‰$) from BC emission inventories for biomass burning in India [*Venkataraman et al.*, 2005]. However, this may introduce some bias to TOC which may include biogenic emissions (primary and secondary); fresh biogenic emissions will have a lower $\Delta^{14}C$ than the ∼30 year old woody biomass which dominates the combustion contributions. A sensitivity analysis of the impact of modern biomass end-member on the $f_{biomass}$ has been previously published [*Gustafsson et al.*, 2009]. Using the $\Delta^{14}C_{sample}$ and the fossil and biomass end-members, the $f_{biomass}$ is then calculated using the relationship below:

$$\Delta^{14}C_{sample} = \Delta^{14}C_{biomass} * f_{biomass} + \Delta^{14}C_{fossil} * (1 - f_{biomass}). \quad (2)$$

2.6. Duration and Mass Normalization of Annual Averages

[16] The sampling was continuous with individual samples comprising a range from three to eighteen days. In order to account for this difference in the duration of the samples when calculating the annual and seasonal averages, a simple normalization was applied. The impact of using the 2008 versus 2009 winter in the annual average has been explored in the Supplemental Materials section S1, but for all annual averages in the text the 2008 average is used. The concentration averages were normalized by the sample volume, which tracks sample duration:

$$C_j = \left(\sum_i C_i v_i\right) / \left(\sum_i v_i\right) \quad (3)$$

where v_i is the sampled air volume for sample i, C_i denotes either the concentration of TOC or SEC, and C_j is the volume-normalized average concentration. These normalized concentration averages were used both in the seasonal and annual average concentrations reported herein, but also as the input concentration for the sample composites used in the F_m normalization and averaging. The radiocarbon averages were normalized by the composite sample concentration and duration:

$$F_j = \left(\sum_i C_i F_i t_i\right) / \left(\sum_i C_j t_i\right) \quad (4)$$

where F_i is the F_m for composite i, C_i denotes either the normalized concentration of TOC or SEC, t is the sampling duration and C_j is the normalized average concentration. Seasonal averaging was designed to parallel seasons determined from back trajectory analysis, when possible.

2.7. Back Trajectory Analysis

[17] Five-day back trajectories (BTs) were completed for MCOH and SINH every 6 h for the entire 15 month campaign using the NOAA HYSPLIT software v4.9 (R. R. Draxler and G. D. Rolph, HYSPLIT (HYbrid Single-Particle Lagrangian Integrated Trajectory) Model access via NOAA ARL READY Website, accessed January 2010, http://ready.arl.noaa.gov/HYSPLIT.php). These individual trajectories were then clustered by month using HYSPLIT, to demonstrate the seasonal trends in source region impacts at each site. The trajectory cluster results are included in the supplementary materials. The cluster means were mapped using indiemapper online mapping software (http://indiemapper.com/) by Axis Maps LLC (http://www.axismaps.com/). Population density for Pakistan, India and Bangladesh was used as the base map for the trajectory clusters at each site (Figures 1 and 2). This data is courtesy of Center for International Earth Science Information Network, Columbia University (Gridded Population of the World Version 3 (GPWv3), Population Density Grids, http://sedac.ciesin.columbia.edu/gpw, accessed 30 August 2011).

[18] The authors acknowledge that the HYSPLIT model has inherent uncertainties including the modeling of terrain height due to the smoothing of complex topography and course resolution in the meteorological model output used to calculate back trajectories. In addition the meteorological model data used to run HYSPLIT hasn't been evaluated at the MCOH and SINH, therefore the results are taken as representative of general trends.

2.8. Geographic Source Assessment

[19] The clustering analysis of the BTs show that the air passing MCOH and SINH during the 2008–2009 campaign can be divided into a few main geographical source regions for each site. By combining the BT analysis with ambient concentration data, it can be determined whether SEC/TOC levels follow any geographical patterns. Such investigations can be done using potential source contribution function analysis or potential emission sensitivity calculations [*Zeng and Hopke*, 1989; *Seibert and Frank*, 2004]. However, they typically utilize long-term data sets with higher time resolution; the current data has a weekly/bi-weekly time resolution. Therefore, potential links between SEC/TOC loadings and geographical origins of the air masses are examined using a measure of the mean TOC or SEC concentration in air from a given geographical source region,

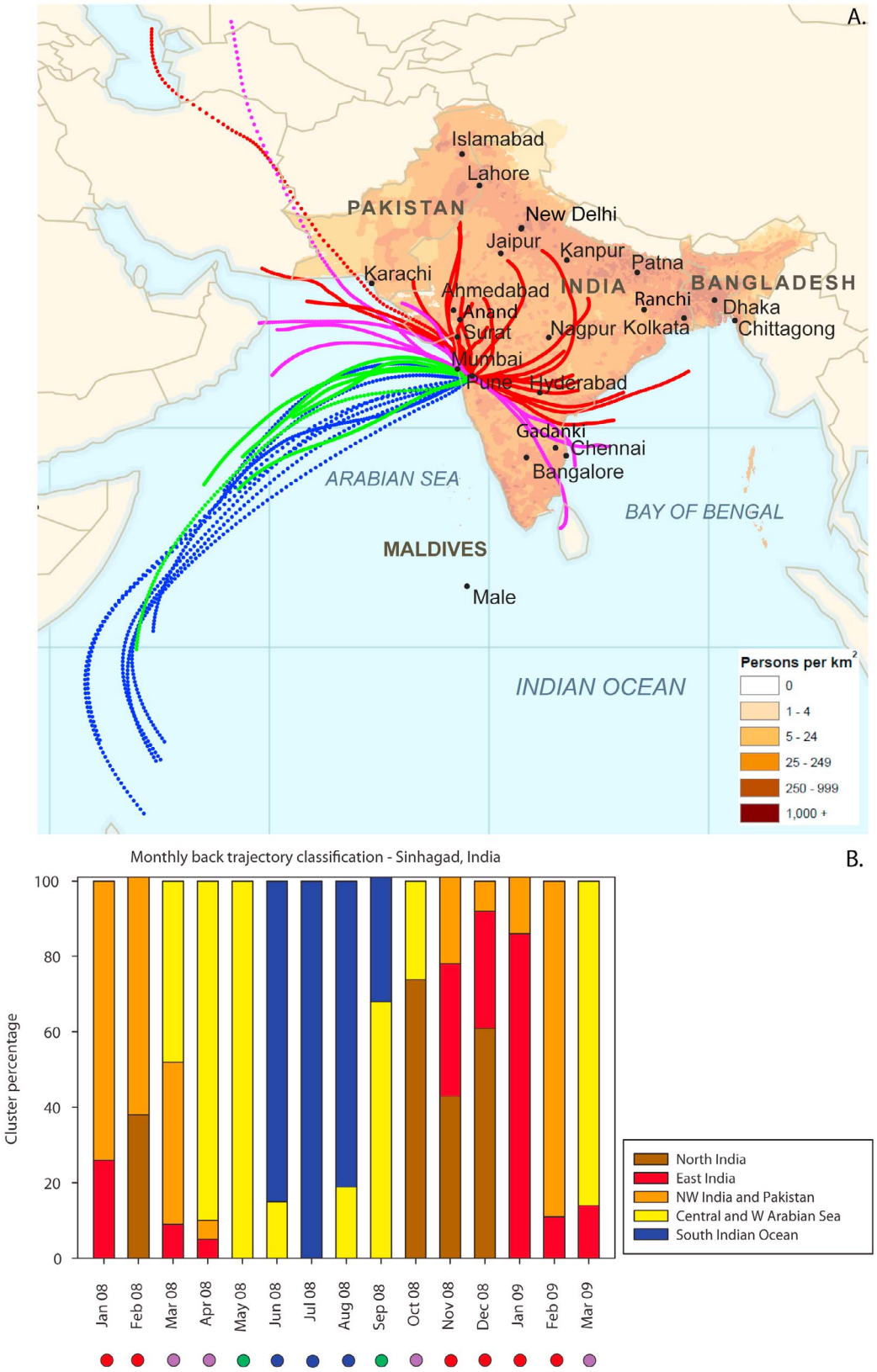

Figure 2. (a) Clustered 6-hourly, 5-day back trajectory means for Sinhagad, India (SINH) for Jan 08–Mar 09 (total n = 1768). The cluster means are colored to depict seasonal differences: winter is red (Jan, Feb, Dec, Nov); winter transition months are purple (Mar, Apr, Oct); pre- and post-monsoon are green (May, Sept); and monsoon is blue (Jun–Aug). (b) Source region classification for clustered back trajectories by month with seasons marked by colored dots.

defined by cluster analysis of BTs. A similar approach was used by *Khan et al.* [2010]. The mean concentration is computed as the mean of TOC or SEC weighted by the fraction air originating from a certain source cluster and the sampling duration:

$$C_{SRj} = \left(\sum_i C_i w_{ji} t_i\right) / \left(\sum_i w_{ji} t_i\right) \quad (5)$$

where w_{ji} is the fraction wind originating from source cluster j for sample number i, C_i denotes the concentration of TOC or SEC, t is the sampling duration, and C_{SRj} is the mean concentration for cluster j.

[20] Since the monsoon season over the Indian subcontinent typically is dominated by winds from the Indian Ocean, this geographic analysis was restricted to the dry season. To exclude small or local variations a cut-off for the fractional influence of certain wind directions was introduced. For MCOH only time points where the summed fractions of air from the BT clusters Bay of Bengal, South India, West India and the Central and W. Arabian Sea exceeded 95% are included in the analysis. This condition is valid for 62% of the total sampling time and 67% of all MCOH samples. For SINH the analysis includes BT clusters for East India, North India, NW India and Pakistan and the Central and W. Arabian Sea. This condition holds for 79% of the total sampling time. To test whether the mean concentration calculated for each source cluster is significantly different than the total mean value for either TOC or SEC, unpaired one-sided T-tests were made.

3. Results and Discussion

3.1. Back Trajectories

[21] Comprehensive back trajectory analysis for both MCOH and SINH was used to characterize the source regions for air masses impacting the 2008–2009 campaign. In addition, population density for Pakistan, India and Bangladesh has been incorporated in Figures 1 and 2 as a proxy for anthropogenic impacts on different BT source regions.

3.1.1. MCOH

[22] The seasonal progression of five-day BT-based air masses is clearly seen with the winter months originating in and around the Indian sub-continent and the summer monsoon air masses originating in the South Indian Ocean (Figure 1a). For the East India clusters, it is reasonable to assume that the Bay of Bengal is heavily impacted by outflow from the Indo-Gangetic Plain (IGP) sources, including high urban emissions from activities associated with regional megacities as well as from rural biomass burning including agricultural and residential practices. This is illustrated by select trajectories from January 2008 and January–February 2009, which can be seen to extend into the IGP (Supplemental Materials). All the Bay of Bengal, East and South Indian BTs also cross densely populated areas of South India in transit to MCOH.

[23] In Figure 1b, a bar graph has been employed to depict the dominant source regions impacting MCOH over the 15-month campaign. The definition of the seasons is based on the BT analysis and is unique for MCOH and SINH. As is expected from the S. Asian monsoon system, the air mass movements showed remarkable stability in the different seasons. This is shown in the January–March clusters, as this time period shows distinct similarity for the two consecutive years of this study. In general, each season has a dominant (i.e., greater than 50%) source region in the cluster analysis. During the dry season from December–January, Bay of Bengal (IGP outflow), East and South Indian source regions have the dominant impact on air masses at MCOH. The W. Indian Margin dominates the clustered back trajectories for November and February, March–April and October are dominated by air masses from the Central and W. Arabian Sea and May–September predominantly experiences air masses from the South Indian Ocean. This analysis is particularly relevant for determining regional differences in sources within S. Asia, i.e., emission source differences between Bay of Bengal/IGP, East India and W. Indian Margin.

[24] Additionally, information can be gleaned about potential impact from the village of Hanimaadhoo on the MCOH measurements. The field site is located on the northern-most tip of the island and there are no back trajectories from the southeast quadrant. Therefore local impact from the airfield at the southern tip of the island or the combustion-related emissions from the village is limited. However, local impact from oceangoing vessels north of the island cannot be ruled out. Recent studies modeling the impact of sulfur emissions from ships highlight a corridor of ship traffic between Hanimaadhoo and India, which may periodically impact the site [*Righi et al.*, 2011].

3.1.2. Sinhagad

[25] The trajectory classification for SINH reveals the same general trend as seen in MCOH, with dry season air masses originating in the Indian subcontinent and then a shift to Central and W Arabian Sea/South Indian Ocean origin in the monsoon season (Figure 2). However, compared to MCOH, there are a few key differences revealed in the SINH BT analysis. There is a shorter period of impact from Indian Ocean-dominated air masses (Figure 2; June–August). During the transition and early dry season, there is a North India influence at SINH (October–December). This switches to East India in January and then NW India and Pakistan in February–March. Similar to MCOH, the Central and W. Arabian Sea influence dominates in March–May and September. For SINH, no cluster means of back trajectories originate from the south quadrant during this 15 month period. At MCOH, all East India and Bay of Bengal air masses cross the southern tip of India, whereas BTs from East and North India cross the less populated central India prior to arrival at Sinhagad and have a shorter transit time. Interestingly, both MCOH and SINH see the most impact from the IGP/East and North India during the onset of the dry season at each site (November–December at SINH, December–January at MCOH), but the source region then shifts to NW India and Pakistan (SINH) and W. Indian Margin (MCOH) as the dry season progresses.

3.1.3. Back Trajectory Heights

[26] The five-day BT heights in the dry season (December–February) are primarily below the Marine Atmospheric Boundary Layer (MABL) as reported in the literature for the Bay of Bengal and Arabian Sea [*Alappattu et al.*, 2008; *Sinha et al.*, 2011]. Figure 3 gives an example of the BT heights

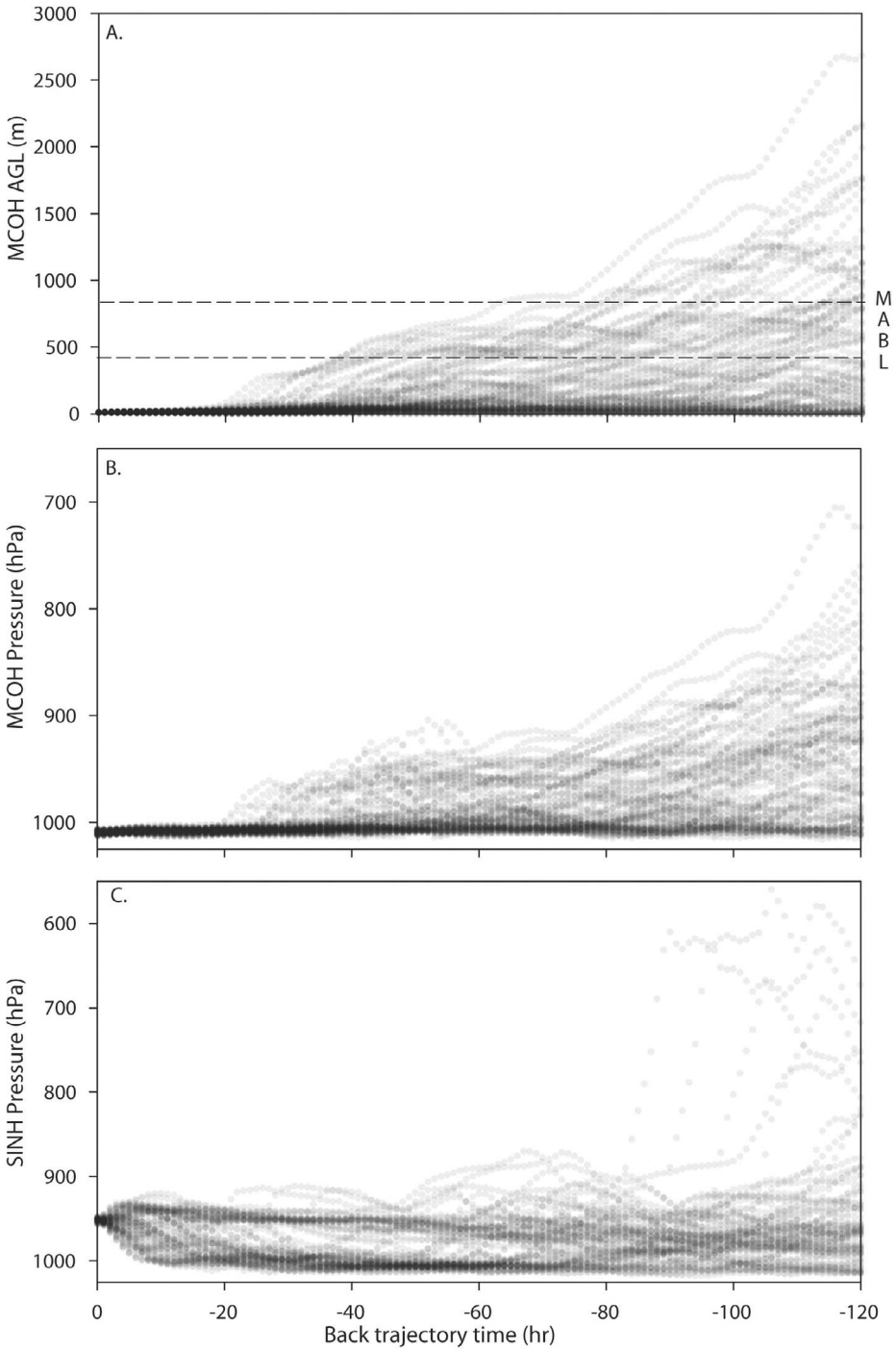

Figure 3. (a) Heights in m (above ground level, AGL) and hPa for 5-day NOAA HYSPLIT back trajectories from (b) Hanimaadhoo, Maldives (MCOH) and (c) Sinhagad, India (SINH). Average marine atmospheric boundary layer heights (MABL) of 400–800 m are depicted. Published continental boundary layer heights are 1–3 km for Dec–Feb for southeastern, eastern and western Indian cities [*Basha and Ratnam*, 2009; *Kumar et al.*, 2011].

during Jan 2008 at both sites; since the MCOH starting height of 10 m above ground level is roughly the same as the above sea level altitude, the height has been plotted in both m and pressure (hPa). There are instances where the BTs rise above the reported average MABL (400–800 m above sea level), however these do not represent the dominant trend. In addition, these higher BTs do fall within the continental India mixing layer height of 1–3 km reported during the

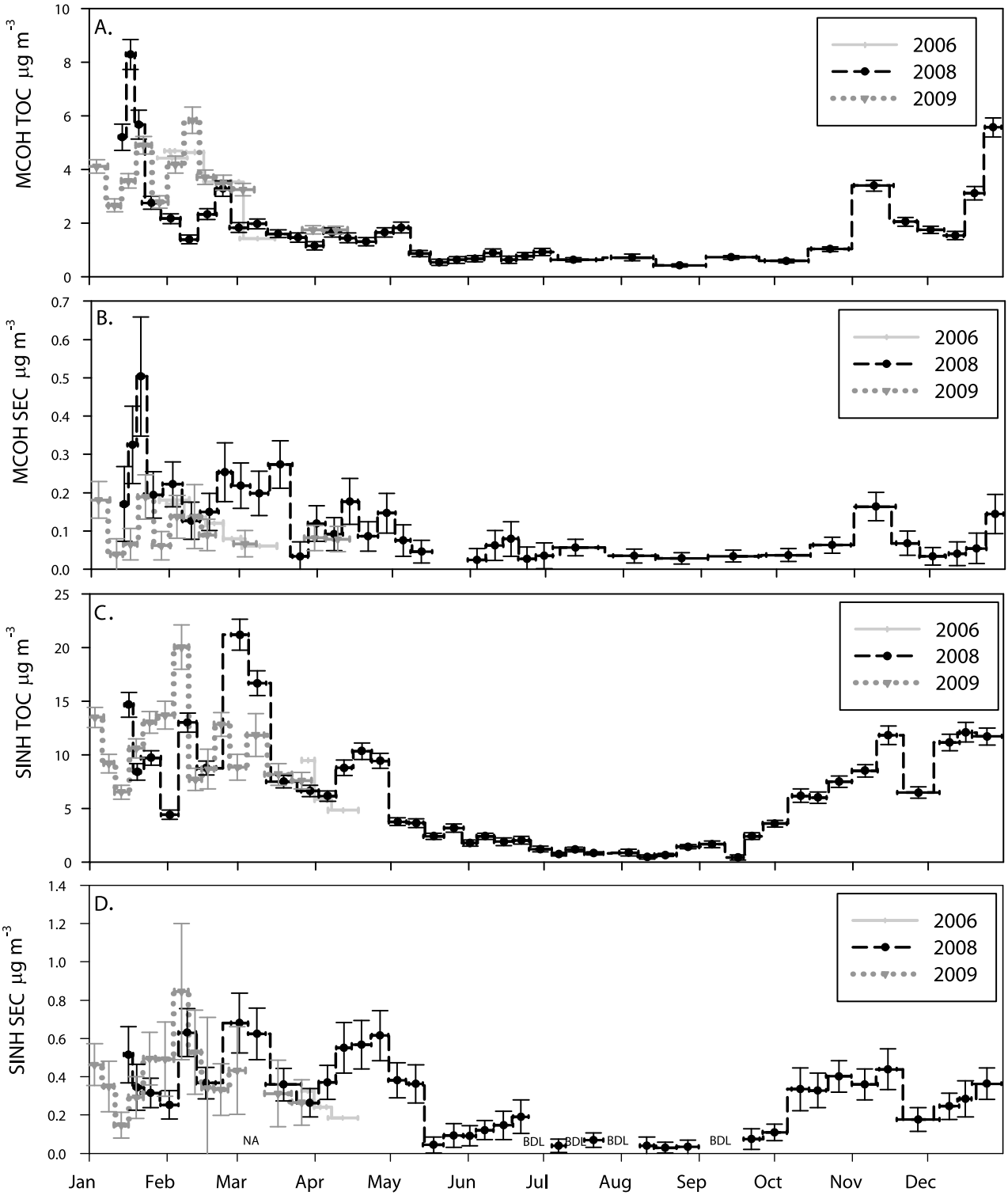

Figure 4. (a and c) Total organic carbon (TOC) and (b and d) soot elemental carbon (SEC) at Hanimaadhoo, Maldives (Figures 4a and 4b) and Sinhagad, India (Figures 4c and 4d). The current study covers 2008–9, with 2006 values previously reported [*Gustafsson et al.*, 2009]. BDL is below detection limit, NA indicates not available. Error bars represent uncertainty.

dry season for southeastern India [*Basha and Ratnam*, 2009] and eastern and western India [*Kumar et al.*, 2011]. With respect to Figure 1, the mean monthly BT clusters for MCOH dominantly travel over the Bay of Bengal, Arabian Sea and Indian Ocean; this makes the MABL height the most relevant. BT heights for SINH in hPa clearly illustrate that typically the airflow rises to the mountain site from lower elevations, dominantly staying below the average continental

Table 1. Mean Concentrations of TOC and SEC by Geographical Source Regions During the Dry Season (C_{SR})[a]

Cluster	C_{TOC} (μg/m^3)	TOC C_{SR} (μg/m^3)	$p_{j,TOC}$	C_{SEC} (μg/m^3)	SEC C_{SR} (μg/m^3)	$p_{j,SEC}$
			MCOH			
Dry season mean	2.1			0.11		
Bay of Bengal		3.9	0.001		0.15	0.08
South India		2.1	0.50		0.08	0.12
W India Margin		2.3	0.32		0.15	0.05
Central and W Arabian Sea		1.2	0.006		0.08	0.10
			SINH			
Dry season mean	8.6			0.33		
North India		8.9	0.44		0.33	0.49
East India		10.8	0.07		0.35	0.36
NW India and Pakistan		11.2	0.05		0.45	0.03
Central and W Arabian Sea		5.4	0.005		0.23	0.04

[a]The p values are also given for difference from dry season means (C_{TOC} and C_{SEC}) by site.

mixing layer height of 1–3 km (~900–700 hPa). BT heights for all months at both sites have been included in the auxiliary material.

3.2. Ambient Concentration of Aerosol Carbon Fractions

3.2.1. Annual Trends

[27] The regional meteorology in S. Asia is driven by the monsoon cycle, which controls annual precipitation patterns and seasonal particulate matter concentrations in both the source regions (India, Bangladesh and Pakistan) and the receptor regions (Maldives and the Indian Ocean) [*Lawrence and Lelieveld*, 2010]. Concentrations are elevated in the dry season and then drop precipitously during the monsoon season due to rainout and influx of "clean" air from the Southern Indian Ocean (Figure 1). The current 15-month data set of carbonaceous aerosol concentration for MCOH and SINH reflect known seasonal variation for the region of South Asia [*Corrigan et al.*, 2006; *Stone et al.*, 2007; *Ram and Sarin*, 2009; *Ram et al.*, 2010]. In general, SEC analysis results in lower concentration than elemental carbon estimated by thermal optical transmittance [*Hammes et al.*, 2007; *Zencak et al.*, 2007; *Gustafsson et al.*, 2009]. The SEC may be regarded as a "macrotracer" of BC; no single method can quantify the entire BC continuum without artifacts but this SEC technique has been demonstrated to isolate the recalcitrant/soot end of the BC spectrum without inducing/including any significant artifacts [*Gustafsson et al.*, 2001; *Elmquist et al.*, 2006; *Hammes et al.*, 2007; *Han et al.*, 2011]. Furthermore, the annual trends for this recalcitrant form of BC, presented here, mimic previously published data sets for other operational definitions of BC for the S. Asian region [*Corrigan et al.*, 2006; *Stone et al.*, 2007].

3.2.1.1. MCOH

[28] The dry season ABC, evidenced by sharp increases in TOC and SEC, commences in November at MCOH and continues through February (Figures 1 and 4). Extremely low concentrations of TOC persist at MCOH during monsoon season from June–October (~0.4–0.8 μg m^{-3}, Figures 1 and 4). Even with the long sampling times, there is variability in the TOC and particularly the SEC concentrations. The relative standard deviation is lower for the seasonal averages versus the annual averages for all but the post-monsoon transition (Oct-Nov), when the ABC is being established. The SEC concentrations for 2006, 2008 and 2009 (Figure 4) are predominantly in the range of 0.08–0.2 μg m^{-3} for January–February and are not significantly different when compared via a two-tailed, heteroscedastic Student's t-test ($p = 0.67$). Relative differences in the SEC to TOC ratio may indicate differences in source contributions, combustion conditions or atmospheric aging. Table S1 in the auxiliary material Text S1 gives the seasonal and annual averages for TOC, SEC and the SEC to TOC ratio. The dry season average from 2008 (7.5%) is much higher than 2009 (2.8%) and 2006 (3.3%) [*Gustafsson et al.*, 2009]. Since SEC is recalcitrant black carbon and likely produced at high combustion temperatures, low temperature biomass combustion would be expected to have lower SC:TOC ratios; this will be discussed further in Section 3.3.1.

3.2.1.2. Sinhagad

[29] At the SINH site in western India, the seasonal average concentrations for TOC and SEC are two-four times higher than MCOH (Figure 4). The monsoon impact on particulate matter concentration is also much shorter in duration. The TOC and SEC concentrations in the post-monsoon period quickly increase from 3.6 μg m^{-3} in September to 6.2 μg m^{-3} in the second week of October for TOC and from 0.1 to 0.3 μg m^{-3} for SEC. For SINH, the SEC to TOC ratio remains more stable than seen at MCOH (auxiliary material Table S1 in Text S1). The March 2006 SEC to TOC [*Gustafsson et al.*, 2009] is more similar to the dry season ratio for the current campaign (3.5%) than the pre-monsoon (4.8%). This indicates minor yearly differences in the onset of monsoon season. The SEC for 2006, 2008 and 2009 for January–April at SINH are in the range of 0.2–0.7 μg m^{-3} and not significantly different at a 95% confidence interval ($p = 0.15$).

3.2.2. Geographic Source Assessment During the Winter Dry Season

[30] The geographic assessment examines whether the source region, as tracked by clustered BTs, impacts the receptor site TOC and SEC concentrations and the SEC to TOC ratio. The mean concentrations and carbon trends from the geographic source assessment are summarized in Table 1 and Figure 5. Overall, significant differences were found to differentiate source regions as compared to the mean dry season concentrations (Table 1). In general, the significance for TOC is higher as compared to the results for SEC, most likely reflecting a larger range in concentrations

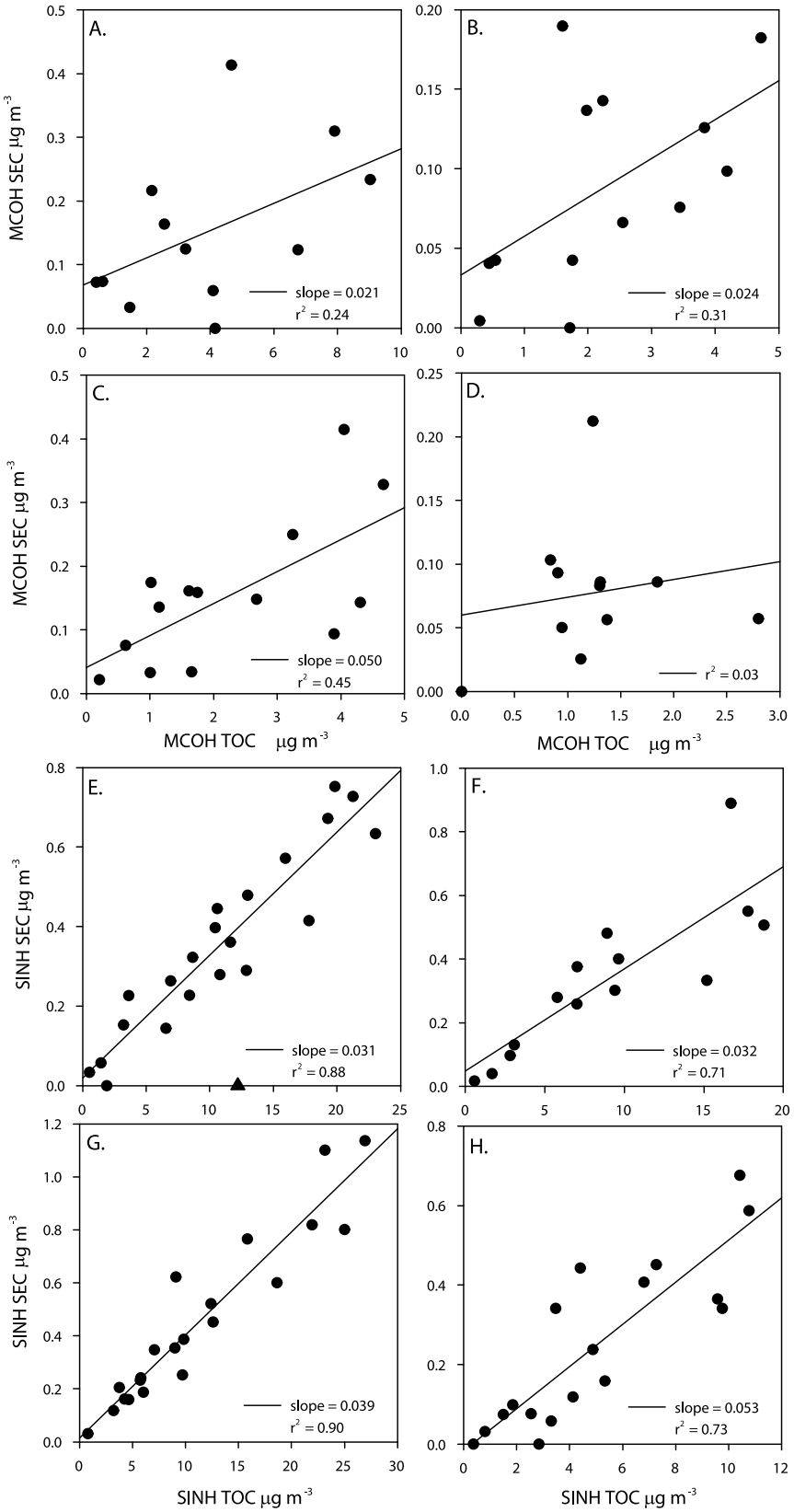

Figure 5. Correlation plots by geographic source region for Hanimaadhoo, Maldives (MCOH) and Sinhagad, India (SINH). (a) Bay of Bengal, (b) South India, (c) W. Indian Margin and (d) Central and W. Arabian Sea are for MCOH, while (e) East India, (f) North India, (g) NW India and Pakistan, and (h) Central and W. Arabian Sea are for SINH. The triangle in Figure 5e was considered an outlier and removed from analysis. r^2 is the Pearson's correlation coefficient.

for TOC. In addition the correlation between SEC and TOC is higher for SINH (Figure 5).

[31] For TOC at MCOH the concentrations are significantly higher for air originating from the Bay of Bengal, 3.9 $\mu g/m^3$, as compared with the mean dry season MCOH levels of 2.1 $\mu g/m^3$. This is expected considering the air over the densely populated IGP is vented into the Bay of Bengal, as discussed in Section 3.1.1. In contrast, air from the Central and W. Arabian Sea has a significantly lower concentration, 1.2 $\mu g/m^3$, compared with the mean MCOH dry season. The TOC associated with the Central and W. Arabian Sea region at MCOH has a much lower concentration of TOC (1.2 $\mu g/m^3$), than the similarly sourced TOC at SINH (5.4 $\mu g/m^3$). However, the air originating from the Central and W. Arabian Sea passes the densely populated region of Mumbai before arriving at SINH. This underscores the difficulty with generalizing the source regions, as the precise routes of transport can have a large impact on concentrations at a given monitoring site.

[32] Air arriving at SINH from NW India and Pakistan and East India has significantly higher TOC concentrations, 10.8 and 11.2 $\mu g\ m^{-3}$compared to the mean dry season concentration of 8.6 $\mu g\ m^{-3}$. In contrast, the TOC from the Central and W. Arabian Sea is significantly lower, 5.4 $\mu g\ m^{-3}$. The TOC associated with the Central and W. Arabian Sea BTs could be influenced by ship emissions, or land-based sources from transport longer than five days. For SEC, similar trends are found, with higher loadings in air from NW India and Pakistan, 0.45 $\mu g\ m^{-3}$, and lower for the Central and W. Arabian Sea, 0.23 $\mu g\ m^{-3}$. The SEC in air from East and North India are not significantly different from the mean dry season concentration of 0.33 $\mu g\ m^{-3}$.

[33] This analysis was also used to examine the SEC to TOC ratio for the different BT source clusters (Figure 5). Using linear regression the SEC to TOC ratios for air arriving at SINH from East India, North India and NW India and Pakistan were ~0.034 with Pearson's correlation coefficients in the range of $0.84 \leq r^2 \leq 0.94$. The same ratio for air from the Central and W. Arabian Sea, disregarding one outlier, is 0.053, with $r^2 = 0.85$. As discussed in the preceding paragraphs, the Central and W Arabian Sea BTs for SINH likely incorporate transit over and impact from Mumbai, whereas the Central and W. Arabian Sea BTs for MCOH are oceanic over the five-day time horizon. For MCOH, the W. Indian Margin had the highest correlation ($r^2 = 0.45$) and a SEC to TOC ratio of 0.05, which most closely parallels the Central and W Arabian Sea ratio for SINH.

3.3. Radiocarbon-Based Source Apportionment and Stable Carbon Isotope Results

[34] Fifteen months of continuous radiocarbon-based source apportionment was achieved for both TOC and SEC components at MCOH and SINH, providing a unique look at the emission source contributions for these S. Asian aerosols (Figure 6). Annual and seasonal averages of the F_m and fraction biomass (by radiocarbon source apportionment) are provided in Table 2.

3.3.1. MCOH

[35] Source apportionment for the year-round campaign of continuous sampling at MCOH revealed that the contribution of biomass combustion to SEC in the Maldives is very consistent, particularly during the dry season (with one single exception in January 2009, Figure 6). Annual-average biomass combustion contribution to SEC is 73 ± 6% at MCOH. The relative standard deviation (r.s.d.) for the annually integrated radiocarbon results (8%) is much lower than the r.s.d. for the annual SEC concentration (86%). This illustrates a consistency in the relative contribution of fossil versus biomass combustion sources throughout the year, indicating that intermittent sources do not dominate the regional SEC load. This is further supported by the $\delta^{13}C$, which also shows high stability for the annual campaign with an annual average of −21.5 ± 1.4‰ (auxiliary material Table S3 in Text S1). The dry season biomass contribution to SEC is the same as the annual average (73 ± 6%). Since the bulk of the mass of SEC that reaches MCOH arrives during the dry season, the annual average is dominated by this dry season biomass combustion. The low SEC to TOC ratio reported in Section 3.2.1.1 for January 2009 corresponds with season-high biomass contribution for SEC of 84% (auxiliary material Table S4 in Text S1). MCOH has a higher contribution from biomass burning to SEC during the monsoon season (June–September), with a maximum 89% biomass burning contribution during Jun 2008 (Figure 6).

[36] For TOC, the biogenic and biomass combustion contribution is also very consistent through the year at 69 ± 5%. There are a few small differences in carbon isotopic composition between the SEC and TOC. The annual-average biomass contribution for TOC is lower than for SEC at MCOH. The range for seasonal average biomass contribution is broader for TOC (13%) than SEC (7%), while the standard deviation is much lower for TOC (1–4%). This is reflective of the impact of seasonal changes in emission sources and geographic source regions. Both TOC and SEC have lower biomass contribution during the dry season and higher biomass contribution during the monsoon season at MCOH. Ambient concentrations are very low during the monsoon season at MCOH, due to the Southern Indian Ocean source region and rainout of particulate matter. However, it may be that this distinct summer signal represents a relatively larger contribution from local sources as prevailing winds and rain scavenging limit any putative long-range transport of PM that prevail in other periods. For MCOH, it is feasible that local biomass burning (including open garbage disposal), primary and secondary biogenic aerosols are larger contributors in the summer monsoon season when the aerosol loading is low.

[37] The $\delta^{13}C$ signature of aerosol TOC and SEC (auxiliary material Table S3 in Text S1) is influenced by the source signature of biogenic and anthropogenic aerosols and atmospheric processing of volatile organic carbon. Source variability is exemplified by the mean $\delta^{13}C$ values observed for C3 and C4 plants (−27‰ and −13‰, respectively [*Smith and Epstein*, 1971]), marine phytoplankton (−21‰ [*Miyazaki et al.*, 2011]), traffic emissions (−25–28‰ [*Huang et al.*, 2006; *Widory*, 2006; *López-Veneroni*, 2009; *Agnihotri et al.*, 2011]) and coal (−24‰ [*Widory*, 2006], −21.75 ± 0.05‰ [*Agnihotri et al.*, 2011]). Oxidation of volatile organic carbon to form secondary aerosols results in a particulate reaction product depleted in ^{13}C relative to the starting material, while oxidation of the aerosol phase may contribute to $\delta^{13}C$ enrichment by preferential removal of lighter carbon isotopes [*Aggarwal and Kawamura*, 2008; *Wang et al.*, 2010]. The yearly mean $\delta^{13}C$ signature for

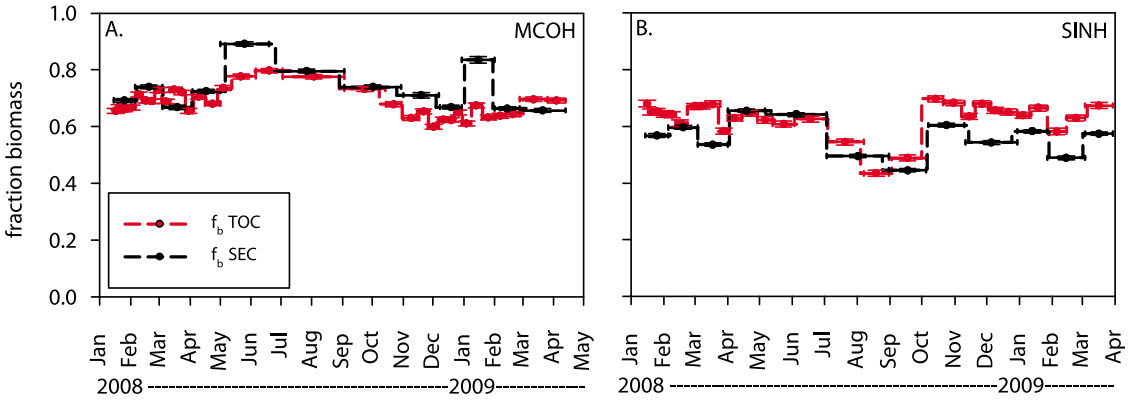

Figure 6. Fraction biomass (f_b) from $\Delta^{14}C$ source apportionment for total organic carbon (TOC) and soot elemental carbon (SEC) at (a) Hanimaadhoo, Maldives (MCOH) and (b) Sinhagad, India (SINH), with analytical error.

MCOH is −21.5 ± 1.4‰ for SEC and −22.8 ± 0.87‰ for TOC, with no clear pronounced annual trend (Tables S3).

3.3.2. Sinhagad

[38] The annual average biomass contribution to SEC at SINH was 59 ± 5%, with a consistent biomass burning predominance throughout the year. SINH is routinely lower in biomass contribution than MCOH (annual average 73 ± 6%). In comparing the BT analysis between sites, MCOH experiences greater impact from South India during the dry season; all the East India BTs cross South India enroute to MCOH. In contrast, the SINH BTs, which also often originate in East India during the dry season, cross central India before reaching SINH. Additionally, many of the BTs which originate in NW India and Pakistan cross Mumbai before reaching SINH, which would likely give a more urban (traffic-related fossil fuel) signature to the carbonaceous aerosol. This difference in source regions may have an impact on the ^{14}C-based source apportionment, resulting in an enhanced fossil signal at SINH.

[39] The biomass contribution to TOC at both sites is nearly identical for the dry season and very similar for the annual average (Table 2). The annual average for SINH is 64 ± 5%. Unlike MCOH, the annual biomass contribution is higher for TOC than SEC at SINH. The $\delta^{13}C$ supports the similarity between MCOH and SINH for TOC, as they are extremely similar and do not have any noticeable seasonal trends. Higher resolution samples may be able to draw out event-based differences in source signals, but the long-term sampling and seasonal averages of this study present a consistent picture in emission sources for TOC. The annual mean SEC $\delta^{13}C$ signal for SINH is −22 ± 0.7‰ (auxiliary material Table S3 in Text S1), mirroring the results from MCOH. In comparison to recent $\delta^{13}C$ for TC (total carbon) for continental Indian urban areas (−24.5 to −26.7‰) and the Bay of Bengal (−24.1 to −27.3‰) [*Agnihotri et al.*, 2011], SINH is somewhat more enriched (annual average of −22.57 ± 0.68‰).

[40] The two sites are similar in the dry season, but the biomass signal at SINH decreases for both TOC and SEC in the peak of the monsoon season (July–September). As discussed for MCOH (Section 3.3.1.), the local signal is likely more dominant in the wet season due to rainout of non-local aerosol. The monsoon season apportionment indicates that in SINH there is less biomass/biofuel burning in the wet

Table 2. Annual and Seasonal Radiocarbon Averages (Concentration-Weighted) for TOC and SEC at Hanimaadhoo, Maldives (MCOH) and Sinhagad, India (SINH)[a]

TOC	F_m	s.d.	f_b (%)	s.d.	SEC	F_m	s.d.	f_b (%)	s.d.
					MCOH				
2008 annual	0.83	0.06	69	5	2008 annual	0.88	0.07	73	6
Dec–Feb[b]	0.78	0.03	65	3	Dec–Feb[b]	0.88	0.07	73	6
Mar–May[b]	0.86	0.04	71	4	Mar–May[b]	0.87	0.10	72	9
Jun–Aug	0.95	0.01	78	1	Jun–Aug	0.96	NA	80	NA
Sept–Nov	0.80	0.05	66	4	Sept–Nov	0.87	0.02	72	1
Jan–Mar 2006[c]			68	3	Jan–Mar 2006[c]			69	6
					SINH				
2008 annual	0.78	0.06	64	5	2008 annual	0.71	0.06	59	5
Nov–Feb[b]	0.77	0.04	64	3	Nov–Feb[b]	0.66	0.05	55	4
Mar–Apr[b]	0.78	0.03	65	3	Mar–Apr[b]	0.72	0.06	60	5
May–Aug	0.71	0.07	59	6	May–Aug	0.73	0.08	61	6
Sept–Oct	0.77	0.10	64	9	Sept–Oct	0.70	0.07	58	6
Mar–Apr 2006[c]			65	2	Mar–Apr 2006[c]			64	3

[a]F_m, fraction modern; f_b, fraction biomass in percent as in equation (1); s.d., standard deviation.
[b]Includes 2008 and 2009.
[c]*Gustafsson et al.* [2009].

season and a relatively larger influence from traffic and fossil fuel sources.

3.3.3. Interannual Variability

[41] The previously published radiocarbon apportionment for the shorter 2006 dry season campaigns at both sites has been included in Table 2 for comparison to the current campaign. For MCOH, the 2006 campaign should be compared to the December–February and March–May averages, while the 2006 SINH campaign can be compared directly to the March–April average. The MCOH-SEC average biomass contribution for 2006 (69 ± 6%) and the current 2008–2009 December–February and March–May (73 ± 6% and 72 ± 9%, respectively) are not statistically different using a two-tailed, heteroscedastic, student's t-test and 95% confidence interval ($p = 0.7$). However, there are slight differences between the 2008 and 2009 seasons for SEC concentrations at MCOH (Figure 4), with higher concentrations extending into transition/pre-monsoon season in March 2008 for SEC. For MCOH TOC, the 2006 average biomass contribution (68 ± 3%) lays directly between the current December–February and March–May averages (65 ± 3% and 71 ± 4%, respectively) and are thus not statistically different ($p = 0.4$). For SINH, the 2006 average biomass contribution for TOC (65 ± 2%) and the 2008 values are nearly identical ($p = 0.4$). As with MCOH, the SEC values show more deviation for SINH; the 2006 average biomass contribution (64 ± 3%) is higher than the 2008 average (60 ± 5%), but is not significantly different ($p = 0.2$). This comparison indicates consistent regional sources for the SEC and TOC for 2006–2009 with about two-thirds of SEC coming from biomass combustion.

4. Implications for Understanding the Emission Sources of Carbonaceous Aerosols in South Asia

[42] The current study provides the first year-round radiocarbon-based source apportionment of combustion aerosols for Asia. The biomass burning contribution to SEC is 73 ± 6% of MCOH and 59 ± 5% at SINH and the biogenic/biomass burning contribution to TOC is 69 ± 5% at MCOH and 64 ± 5% at SINH. These mass and duration-weighted annual averages reveal a somewhat greater divergence in the biomass contribution to SEC at the two regional sites than was apparent in the much shorter 2006 campaign [*Gustafsson et al.*, 2009]. In this case, the support of the back trajectory analysis indicates that differences in source regions likely explain the difference in SEC biomass contribution in the dry season, with air masses to MCOH crossing South India while SINH is experiencing more influence from Central India. This highlights the importance of long-term campaigns to increase the accuracy of the source estimates and enable better comparability with emissions inventory-based assessments.

[43] Encouragingly, the current year-round observation-based campaign does compare well with published BC emissions inventories for outflow of carbonaceous aerosols from S. Asia. Several published inventories suggest that biomass/biofuel burning contributes roughly 70–75% of the total BC [*Reddy and Venkataraman*, 2002a, 2002b; *Bond et al.*, 2004; *Venkataraman et al.*, 2005], which correspond closely to the fraction biomass for SEC seen in the annual MCOH reported here. Dickerson has a reported range for biomass/biofuel burning contribution based on CO emissions inventory of 55–88% [*Dickerson et al.*, 2002], which would include the apportionment results from both SINH and MCOH. The current study lies closer to the biomass versus fossil fuel split estimated in these bottom-up emission inventories than reported for most other top-down receptor modeling studies [*Novakov et al.*, 2000; *Mayol-Bracero et al.*, 2002; *Lawrence and Lelieveld*, 2010], which tend to estimate a dominant contribution from fossil fuel combustion. In contrast, *Guazzotti et al.* [2003] in their receptor modeling study, using time-of-flight mass spectrometer measurements, reported a biomass contribution of 74 ± 9% to total carbonaceous particles at MCOH.

[44] While the current study provides an observation-based, annual-average source apportionment of regional background carbonaceous aerosols for the S. Asian region, many additional questions remain. The results of the back trajectory analysis and source region attribution of SEC and TOC highlight that higher time resolution radiocarbon analysis of BC in the dry season outflow are needed to resolve the source apportionment by region. Additional source-diagnostic markers, such as organic molecular markers [*Stone et al.*, 2007; *Sheesley et al.*, 2011], are needed in concert with carbon isotopes to resolve among additional combustion sources. Finally, other carbonaceous aerosol components such as water-soluble organic carbon (relevant for cloud forming potential) and thermo-optical transmission based elemental carbon, may yield a more comprehensive picture of the sources of climate-affecting aerosol carbon in this dynamically changing region of Asia.

[45] **Acknowledgments.** The authors would like to thank the UNEP-RRC and EPA of the Republic of the Maldives for joint operation of MCOH, especially Ibrahim Muhammed, Abdul Muhsin Ramiz, Adam Saleem, Sharafulla Thoha and Faruhaadoo Moosa of the Maldivian EPA and Maheswar Rupakheti of UNEP-RRC. The authors would like to thank the Indian Institute for Tropical Meteorology in Pune, India for supporting the site at Sinhagad. The authors appreciate constructive comments on earlier versions of this work from Caroline Leck and Henning Rodhe. The authors would like to acknowledge support from the Swedish funding agencies Formas and SIDA. Ö.G. also acknowledges support as an Academy Researcher at the Royal Academy of Sciences through a grant from the Knut and Alice Wallenberg Foundation. A.A. acknowledges the Knut and Alice Wallenberg Foundation for financial support.

References

Adhikary, B., G. R. Carmichael, Y. Tang, L. R. Leung, Y. Qian, J. J. Schauer, E. A. Stone, V. Ramanathan, and M. V. Ramana (2007), Characterization of the seasonal cycle of south Asian aerosols: A regional-scale modeling analysis, *J. Geophys. Res.*, *112*, D22S22, doi:10.1029/2006JD008143.

Aggarwal, S. G., and K. Kawamura (2008), Molecular distributions and stable carbon isotopic compositions of dicarboxylic acids and related compounds in aerosols from Sapporo, Japan: Implications for photochemical aging during long-range atmospheric transport, *J. Geophys. Res.*, *113*, D14301, doi:10.1029/2007JD009365.

Agnihotri, R., T. K. Mandal, S. G. Karapurkar, M. Naja, R. Gadi, Y. N. Ahammmed, A. Kumar, T. Saud, and M. Saxena (2011), Stable carbon and nitrogen isotopic composition of bulk aerosols over India and northern Indian Ocean, *Atmos. Environ.*, *45*, 2828–2835, doi:10.1016/j.atmosenv.2011.03.003.

Alappattu, D. P., D. B. Subrahamanyam, P. K. Kunhikrishnan, K. M. Somayaji, G. S. Bhat, R. Venkatesan, C. B. S. Dutt, A. B. Singh, V. K. Soni, and A. S. Tripathi (2008), On the marine atmospheric boundary layer characteristics over Bay of Bengal and Arabian Sea during the Integrated Campaign for Aerosols, gases and Radiation Budget (ICARB), *J. Earth Syst. Sci.*, *117*, 281–291, doi:10.1007/s12040-008-0031-0.

Andersson, A., R. J. Sheesley, M. Krusa, C. Johansson, and O. Gustafsson (2011), ^{14}C-based source assessment of soot aerosols in Stockholm

and the Swedish EMEP-Aspvreten regional background site, *Atmos. Environ.*, *45*, 215–222, doi:10.1016/j.atmosenv.2010.09.015.

Basha, G., and M. V. Ratnam (2009), Identification of atmospheric boundary layer height over a tropical station using high-resolution radiosonde refractivity profiles: Comparison with GPS radio occultation measurements, *J. Geophys. Res.*, *114*, D16101, doi:10.1029/2008JD011692.

Bench, G., and P. Herckes (2004), Measurement of contemporary and fossil carbon contents of $PM_{2.5}$ aerosols: Results from Turtleback Dome, Yosemite National Park, *Environ. Sci. Technol.*, *38*, 2424–2427, doi:10.1021/es035161s.

Bond, T. C., D. G. Streets, K. F. Yarber, S. M. Nelson, J. H. Woo, and Z. Klimont (2004), A technology-based global inventory of black and organic carbon emissions from combustion, *J. Geophys. Res.*, *109*, D14203, doi:10.1029/2003JD003697.

Budhavant, K. B., P. S. P. Rao, P. D. Safai, and K. Ali (2011), Influence of local sources on rainwater chemistry over Pune region, India, *Atmos. Res.*, *100*, 121–131, doi:10.1016/j.atmosres.2011.01.004.

Cole, M. A., and E. Neumayer (2004), Examining the impact of demographic factors on air pollution, *Popul. Environ.*, *26*, 5–21, doi:10.1023/B:POEN.0000039950.85422.eb.

Corrigan, C. E., V. Ramanathan, and J. J. Schauer (2006), Impact of monsoon transitions on the physical and optical properties of aerosols, *J. Geophys. Res.*, *111*, D18208, doi:10.1029/2005JD006370.

Coz, E., and C. Leck (2011), Morphology and state of mixture of atmospheric soot aggregates during the winter season over Southern Asia—A quantitative approach, *Tellus, Ser. B*, *63*, 107–116, doi:10.1111/j.1600-0889.2010.00513.x.

Dickerson, R. R., M. O. Andreae, T. Campos, O. L. Mayol-Bracero, C. Neusuess, and D. G. Streets (2002), Analysis of black carbon and carbon monoxide observed over the Indian Ocean: Implications for emissions and photochemistry, *J. Geophys. Res.*, *107*(D19), 8017, doi:10.1029/2001JD000501.

Elmquist, M., G. Cornelissen, Z. Kukulska, and O. Gustafsson (2006), Distinct oxidative stabilities of char versus soot black carbon: Implications for quantification and environmental recalcitrance, *Global Biogeochem. Cycles*, *20*, GB2009, doi:10.1029/2005GB002629.

Granat, L., J. E. Engstrom, S. Praveen, and H. Rodhe (2010), Light absorbing material (soot) in rainwater and in aerosol particles in the Maldives, *J. Geophys. Res.*, *115*, D16307, doi:10.1029/2009JD013768.

Guazzotti, S. A., et al. (2003), Characterization of carbonaceous aerosols outflow from India and Arabia: Biomass/biofuel burning and fossil fuel combustion, *J. Geophys. Res.*, *108*(D15), 4485, doi:10.1029/2002JD003277.

Gustafsson, O., F. Haghseta, C. Chan, J. MacFarlane, and P. M. Gschwend (1997), Quantification of the dilute sedimentary soot phase: Implications for PAH speciation and bioavailability, *Environ. Sci. Technol.*, *31*, 203–209, doi:10.1021/es960317s.

Gustafsson, Ö., T. D. Bucheli, Z. Kukulska, M. Andersson, C. Largeau, J. N. Rouzaud, C. M. Reddy, and T. I. Eglinton (2001), Evaluation of a protocol for the quantification of black carbon in sediments, *Global Biogeochem. Cycles*, *15*, 881–890, doi:10.1029/2000GB001380.

Gustafsson, O., M. Krusa, Z. Zencak, R. J. Sheesley, L. Granat, E. Engstrom, P. S. Praveen, P. S. P. Rao, C. Leck, and H. Rodhe (2009), Brown clouds over South Asia: Biomass or fossil fuel combustion?, *Science*, *323*, 495–498, doi:10.1126/science.1164857.

Hammes, K., et al. (2007), Comparison of quantification methods to measure fire-derived (black/elemental) carbon in soils and sediments using reference materials from soil, water, sediment and the atmosphere, *Global Biogeochem. Cycles*, *21*, GB3016, doi:10.1029/2006GB002914.

Han, Y. M., J. J. Cao, B. Z. Yan, T. C. Kenna, Z. D. Jin, Y. Cheng, J. C. Chow, and Z. S. An (2011), Comparison of elemental carbon in lake sediments measured by three different methods and 150-year pollution history in eastern China, *Environ. Sci. Technol.*, *45*, 5287–5293, doi:10.1021/es103518c.

Holecek, J. C., M. T. Spencer, and K. A. Prather (2007), Analysis of rainwater samples: Comparison of single particle residues with ambient particle chemistry from the northeast Pacific and Indian oceans, *J. Geophys. Res.*, *112*, D22S24, doi:10.1029/2006JD008269.

Huang, L., J. R. Brook, W. Zhang, S. M. Li, L. Graham, D. Ernst, A. Chivulescu, and G. Lu (2006), Stable isotope measurements of carbon fractions (OC/EC) in airborne particulate: A new dimension for source characterization and apportionment, *Atmos. Environ.*, *40*, 2690–2705, doi:10.1016/j.atmosenv.2005.11.062.

Khan, A. J., J. J. Li, V. A. Dutkiewicz, and L. Husain (2010), Elemental carbon and sulfate aerosols over a rural mountain site in the northeastern United States: Regional emissions and implications for climate change, *Atmos. Environ.*, *44*, 2364–2371, doi:10.1016/j.atmosenv.2010.03.025.

Kirchstetter, T. W., T. Novakov, and P. V. Hobbs (2004), Evidence that the spectral dependence of light absorption by aerosols is affected by organic carbon, *J. Geophys. Res.*, *109*, D21208, doi:10.1029/2004JD004999.

Kumar, M., A. Kumar, C. Mallik, N. C. Mahanti, and A. M. Shekh (2011), Daytime boundary layer behavior over eastern region (per-humid climate) and western regions (semi-arid climate) of India: A case study, *Meteorol. Atmos. Phys.*, *111*, 55–64, doi:10.1007/s00703-010-0116-6.

Lawrence, M. G., and J. Lelieveld (2010), Atmospheric pollutant outflow from southern Asia: A review, *Atmos. Chem. Phys.*, *10*, 11,017–11,096, doi:10.5194/acp-10-11017-2010.

Lelieveld, J., et al. (2001), The Indian Ocean Experiment: Widespread air pollution from South and Southeast Asia, *Science*, *291*, 1031–1036, doi:10.1126/science.1057103.

López-Veneroni, D. (2009), The stable carbon isotope composition of $PM_{2.5}$ and PM_{10} in Mexico City metropolitan area air, *Atmos. Environ.*, *43*, 4491–4502, doi:10.1016/j.atmosenv.2009.06.036.

Mandalakis, M., O. Gustafsson, T. Alsberg, A. L. Egeback, C. M. Reddy, L. Xu, J. Klanova, I. Holoubek, and E. G. Stephanou (2005), Contribution of biomass burning to atmospheric polycyclic aromatic hydrocarbons at three European background sites, *Environ. Sci. Technol.*, *39*, 2976–2982, doi:10.1021/es048184v.

Mayol-Bracero, O. L., R. Gabriel, M. O. Andreae, T. W. Kirchstetter, T. Novakov, J. Ogren, P. Sheridan, and D. G. Streets (2002), Carbonaceous aerosols over the Indian Ocean during the Indian Ocean Experiment (INDOEX): Chemical characterization, optical properties, and probable sources, *J. Geophys. Res.*, *107*(D19), 8030, doi:10.1029/2000JD000039.

Menon, S., J. Hansen, L. Nazarenko, and Y. F. Luo (2002), Climate effects of black carbon aerosols in China and India, *Science*, *297*, 2250–2253, doi:10.1126/science.1075159.

Miyazaki, Y., K. Kawamura, J. Jung, H. Furutani, and M. Uematsu (2011), Latitudinal distributions of organic nitrogen and organic carbon in marine aerosols over the western North Pacific, *Atmos. Chem. Phys.*, *11*, 3037–3049, doi:10.5194/acp-11-3037-2011.

Momin, G. A., K. Ali, P. S. P. Rao, P. D. Safai, D. M. Chate, P. S. Praveen, H. Rodhe, and L. Granat (2005), Study of chemical composition of rainwater at an urban (Pune) and a rural (Sinhagad) location in India, *J. Geophys. Res.*, *110*, D08302, doi:10.1029/2004JD004789.

Neusuess, C., T. Gnauk, A. Plewka, H. Herrmann, and P. K. Quinn (2002), Carbonaceous aerosol over the Indian Ocean: OC/EC fractions and selected specifications from size-segregated onboard samples, *J. Geophys. Res.*, *107*(D19), 8031, doi:10.1029/2001JD000327.

Novakov, T., M. O. Andreae, R. Gabriel, T. W. Kirchstetter, O. L. Mayol-Bracero, and V. Ramanathan (2000), Origin of carbonaceous aerosols over the tropical Indian Ocean: Biomass burning or fossil fuels?, *Geophys. Res. Lett.*, *27*, 4061–4064, doi:10.1029/2000GL011759.

O'Neill, B. C., M. Dalton, R. Fuchs, L. W. Jiang, S. Pachauri, and K. Zigova (2010), Global demographic trends and future carbon emissions, *Proc. Natl. Acad. Sci. U. S. A.*, *107*, 17,521–17,526, doi:10.1073/pnas.1004581107.

Pucher, J., Z. R. Peng, N. Mittal, Y. Zhu, and N. Korattyswaroopam (2007), Urban transport trends and policies in China and India: Impacts of rapid economic growth, *Transp. Rev.*, *27*, 379–410, doi:10.1080/01441640601089988.

Raju, M. P., P. D. Safai, P. S. P. Rao, P. C. S. Devara, and K. B. Budhavant (2011), Seasonal characteristics of black carbon aerosols over a high altitude station in southwest India, *Atmos. Res.*, *100*, 103–110, doi:10.1016/j.atmosres.2011.01.006.

Ram, K., and M. M. Sarin (2009), Absorption coefficient and site-specific mass absorption efficiency of elemental carbon in aerosols over urban, rural, and high-altitude sites in India, *Environ. Sci. Technol.*, *43*, 8233–8239, doi:10.1021/es9011542.

Ram, K., M. M. Sarin, and S. N. Tripathi (2010), Inter-comparison of thermal and optical methods for determination of atmospheric black carbon and attenuation coefficient from an urban location in northern India, *Atmos. Res.*, *97*, 335–342, doi:10.1016/j.atmosres.2010.04.006.

Ramana, M. V., and V. Ramanathan (2006), Abrupt transition from natural to anthropogenic aerosol radiative forcing: Observations at the ABC-Maldives Climate Observatory, *J. Geophys. Res.*, *111*, D20207, doi:10.1029/2006JD007063.

Ramana, M. V., V. Ramanathan, Y. Feng, S. C. Yoon, S. W. Kim, G. R. Carmichael, and J. J. Schauer (2010), Warming influenced by the ratio of black carbon to sulphate and the black-carbon source, *Nat. Geosci.*, *3*, 542–545, doi:10.1038/ngeo918.

Ramanathan, V., and G. Carmichael (2008), Global and regional climate changes due to black carbon, *Nat. Geosci.*, *1*, 221–227, doi:10.1038/ngeo156.

Ramanathan, V., and P. J. Crutzen (2003), New directions: Atmospheric brown "clouds," *Atmos. Environ.*, *37*, 4033–4035, doi:10.1016/S1352-2310(03)00536-3.

Ramanathan, V., P. J. Crutzen, J. T. Kiehl, and D. Rosenfeld (2001), Atmosphere—Aerosols, climate, and the hydrological cycle, *Science*, *294*, 2119–2124, doi:10.1126/science.1064034.

Reddy, M. S., and C. Venkataraman (2002a), Inventory of aerosol and sulphur dioxide emissions from India: I - Fossil fuel combustion, *Atmos. Environ.*, *36*, 677–697, doi:10.1016/S1352-2310(01)00463-0.

Reddy, M. S., and C. Venkataraman (2002b), Inventory of aerosol and sulphur dioxide emissions from India. Part II - Biomass combustion, *Atmos. Environ.*, *36*, 699–712, doi:10.1016/S1352-2310(01)00464-2.

Rengarajan, R., M. M. Sarin, and A. K. Sudheer (2007), Carbonaceous and inorganic species in atmospheric aerosols during wintertime over urban and high-altitude sites in North India, *J. Geophys. Res.*, *112*, D21307, doi:10.1029/2006JD008150.

Righi, M., C. Klinger, V. Eyring, J. Hendricks, A. Lauer, and A. Petzold (2011), Climate impact of biofuels in shipping: Global model studies of the aerosol indirect effect, *Environ. Sci. Technol.*, *45*, 3519–3525, doi:10.1021/es1036157.

Salam, A., H. Bauer, K. Kassin, S. M. Ullah, and H. Puxbaum (2003), Aerosol chemical characteristics of an island site in the Bay of Bengal (Bhola-Bangladesh), *J. Environ. Monit.*, *5*, 483–490, doi:10.1039/b212521h.

Sandradewi, J., A. S. H. Prevot, S. Szidat, N. Perron, M. R. Alfarra, V. A. Lanz, E. Weingartner, and U. Baltensperger (2008), Using aerosol light absorption measurements for the quantitative determination of wood burning and traffic emission contributions to particulate matter, *Environ. Sci. Technol.*, *42*, 3316–3323, doi:10.1021/es702253m.

Seibert, P., and A. Frank (2004), Source-receptor matrix calculation with a Lagrangian particle dispersion model in backward mode, *Atmos. Chem. Phys.*, *4*, 51–63, doi:10.5194/acp-4-51-2004.

Sheesley, R. J., A. Andersson, and Ö. Gustafsson (2011), Source characterization of organic aerosols using Monte Carlo source apportionment of PAHs at two South Asian receptor sites, *Atmos. Environ.*, *45*, 3874–3881, doi:10.1016/j.atmosenv.2011.01.031.

Sinha, P. R., R. K. Manchanda, J. V. Subbarao, U. C. Dumka, S. Sreenivasan, S. S. Babu, and K. K. Moorthy (2011), Spatial distribution and vertical structure of the MABL aerosols over Bay of Bengal during winter: Results from W-ICARB experiment, *J. Atmos. Sol. Terr. Phys.*, *73*, 430–438, doi:10.1016/j.jastp.2010.10.011.

Smith, B. N., and S. Epstein (1971), Two categories of $^{13}C/^{12}C$ ratios for higher plants, *Plant Physiol.*, *47*, 380–384, doi:10.1104/pp.47.3.380.

Stone, E. A., G. C. Lough, J. J. Schauer, P. S. Praveen, C. E. Corrigan, and V. Ramanathan (2007), Understanding the origin of black carbon in the atmospheric brown cloud over the Indian Ocean, *J. Geophys. Res.*, *112*, D22S23, doi:10.1029/2006JD008118.

Stuiver, M., and H. A. Polach (1977), Reporting of ^{14}C data—Discussion, *Radiocarbon*, *19*, 355–363.

Szidat, S., T. M. Jenk, H. A. Synal, M. Kalberer, L. Wacker, I. Hajdas, A. Kasper-Giebl, and U. Baltensperger (2006), Contributions of fossil fuel, biomass-burning, and biogenic emissions to carbonaceous aerosols in Zurich as traced by ^{14}C, *J. Geophys. Res.*, *111*, D07206, doi:10.1029/2005JD006590.

U. N. Environmental Programme (UNEP) (2008), Atmospheric brown clouds: Regional assessment report with focus on Asia, summary report, 44 pp., Nairobi, Kenya.

Venkataraman, C., G. Habib, A. Eiguren-Fernandez, A. H. Miguel, and S. K. Friedlander (2005), Residential biofuels in south Asia: Carbonaceous aerosol emissions and climate impacts, *Science*, *307*, 1454–1456, doi:10.1126/science.1104359.

Wang, G., M. Xie, S. Hu, S. Gao, E. Tachibana, and K. Kawamura (2010), Dicarboxylic acids, metals and isotopic compositions of C and N in atmospheric aerosols from inland China: Implications for dust and coal burning emission and secondary aerosol formation, *Atmos. Chem. Phys.*, *10*, 6087–6096, doi:10.5194/acp-10-6087-2010.

Widory, D. (2006), Combustibles, fuels and their combustion products: A view through carbon isotopes, *Combust. Theory Modell.*, *10*, 831–841, doi:10.1080/13647830600720264.

Zencak, Z., M. Elmquist, and O. Gustafsson (2007), Quantification and radiocarbon source apportionment of black carbon in atmospheric aerosols using the CTO-375 method, *Atmos. Environ.*, *41*, 7895–7906, doi:10.1016/j.atmosenv.2007.06.006.

Zeng, Y., and P. K. Hopke (1989), A study of the sources of acid precipitation in Ontario, Canada, *Atmos. Environ.*, *23*, 1499–1509, doi:10.1016/0004-6981(89)90409-5.